ARTICLE

OBC
www.rsc.org/obc

Ring currents in the porphyrins: π shielding, delocalisation pathways and the central cation

Erich Steiner,[a] Alessandro Soncini[b] and Patrick W. Fowler*[c]

[a] *School of Biosciences, University of Exeter, Exeter, UK EX4 4QD*

[b] *Dipartimento di Chimica, Università degli Studi di Modena e Reggio Emilia, via Campi 183, 41100 Modena, Italy*

[c] *Department of Chemistry, University of Sheffield, Sheffield, UK S3 7HF*

Received 22nd August 2005, Accepted 9th September 2005
First published as an Advance Article on the web 13th October 2005

It is shown that the ipsocentric orbital-based model explains how the charge of the central cation drives the delocalisation pathway in metalloporphyrins. A positive charge $+Ze$ at the centre of the porphin ring gives rise to a two-way radial transfer of charge within the π structure of the porphin macrocycle. This manifests itself in a change of pathway of the global π current, as Z increases from $Z = 0$, from an inner- through a bifurcated- to an outer-pathway. Changes of pathway can be interpreted in terms of a specific π shielding effect whereby electrons in high-lying π orbitals are screened from the central charge by the electrons in lower-lying orbitals of the same symmetry. These changes in π structure are essentially independent of accompanying changes in the σ structure.

1. Introduction

An understanding of the nature and origin of the global π ring current in the porphin macrocycle of porphyrins has recently been obtained[1–4] within molecular orbital theory by means of coupled Hartree–Fock calculations in the ipsocentric formulation.[5–8] The present paper will show that this approach also explains the spatial distribution of current and its dependence on a central charge, predicting a systematic variation of delocalisation pathway with a central cation in metalloporphyrins and related systems. We show that the dependence of the current density distribution on the central charge can be explained in detail by adopting the principle (i) that changes in current densities follow changes in charge densities, or more precisely, transition densities, and the hypothesis (ii) that, in the presence of a central charge, there exists a π shielding effect whereby electrons in high-lying π orbitals of each symmetry type are shielded from the centre by the lower-lying orbitals of the same symmetry. These considerations apply to a wide range of known molecules, with almost every metal in the periodic table forming a central complex with porphyrins[9] or with the structurally similar phthalocyanines,[10] as well as with a variety of expanded and contracted porphyrins,[11] some in several oxidation states from +1 to +6.

Representative current maps are illustrated in Fig. 1 for (a) the dianion macrocycle in (neutral) magnesium porphin, [MgP], and (b) the neutral macrocycle in the dication $[MgP]^{2+}$. Both display clear global ring currents, the blue and red colours highlighting the difference between the oppositely circulating diatropic (diamagnetic) and paratropic (paramagnetic) currents (see also ref. 3). An indication of current strength is given by its largest magnitude in the plotting plane, and by this measure, the porphin π ring current is twice as strong as that of benzene.

Several delocalisation pathways can be devised for the flow of π electrons through the 24-site conjugated π system of the porphin macrocycle,[4] and the current density maps of Fig. 1 suggest that the total, *bifurcated* flow can be analysed as a combination of 16-site inner and 20-site outer pathways. In neutral [MgP], the number of contributing π electrons is nominally 18 (inner) and 22 (outer), both consistent with Hückel's $(4n + 2)$ rule for aromaticity of a monocycle. In the dication, $[MgP]^{2+}$, the counts of 16 and 20 are consistent with the $4n$ rule for antiaromaticity. An alternative analysis considers a combination of the two orthogonal 18-site pathways conventionally invoked to represent π delocalisation in free-base porphin,[13] which carry 18 π electrons in [MgP] and 16 in $[MgP]^{2+}$. Historically, this was the basis for the interpretation

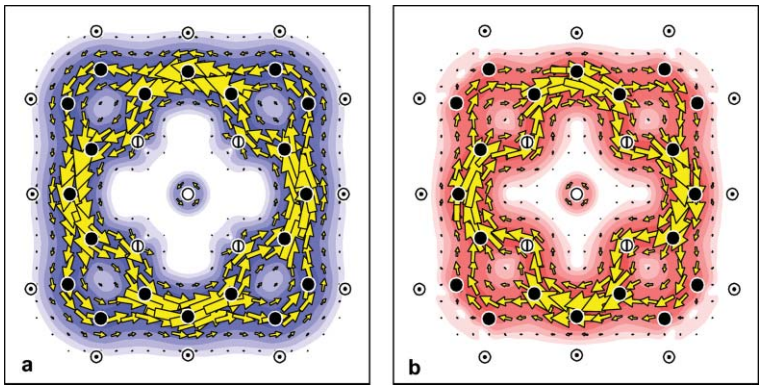

Fig. 1 π Total current density maps in magnesium porphin: (a) neutral [MgP], (b) dication $[MgP]^{2+}$, calculated at the ipsocentric CTOCD-DZ/6-31G**//RHF/6-31G** level and plotted at $1a_0$ from the nuclear plane, close to the maxima of the π current and charge densities. Colours indicate the type and intensity of the global ring current: blue for diatropic, red for paratropic. Diatropic circulation is anticlockwise, paratropic clockwise. Maximum currents in the plotting plane are $j_{max} = 0.17$ a.u. in [MgP], 0.15 a.u. in $[MgP]^{2+}$, where 0.08 a.u. is the value for benzene. Atom symbols are Dalton's:[12] circle with dot for H, solid circle for C, bisected circle for N.

DOI:10.1039/b511913h

of the electronic spectra of porphyrins in terms of frontier π–π* orbital transitions (see ref. 4 and references cited therein).

The patterns of frontier π orbital levels of the macrocycle in [MgP] and $[MgP]^{2+}$ are shown in Fig. 2, with indications of the orbital transitions allowed under electric- and magnetic-dipole selection rules. In D_{4h} [MgP], $1a_{1u}$ and $3a_{2u}$ (HOMO and HOMO′) form a near-degenerate pair, with nodal symmetry corresponding to angular momentum quantum number $\lambda = 4$. The degenerate $4e_g$ LUMO pair has one more node ($\lambda = 5$). The $\Delta\lambda = 1$ HOMO–LUMO transitions are therefore expected to dominate the electronic spectrum of the molecule. Gouterman[14] has shown that a good description of the two lowest-lying E_u excited states is obtained by interaction of two orbital configurations (a_{1u}, e_g) and (a_{2u}, e_g). This 'four-orbital model' provides a realistic interpretation of the relative intensities of the transitions, with weak absorption (Q bands) in the visible and intense Soret absorption (B bands) in the near-UV.

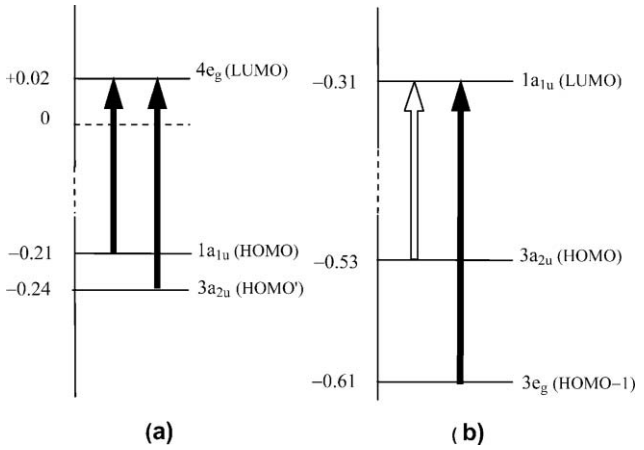

Fig. 2 Schematic patterns of frontier π orbital energy levels in (a) [MgP] and (b) $[MgP]^{2+}$. The energies (a.u.) are for D_{4h} RHF-optimised geometries within the 6-31G** Gaussian basis. Also shown are the occupied-to-unoccupied orbital transitions allowed by electric-dipole (black arrows) and magnetic-dipole (white arrow) selection rules.

The model of the spectrum is relevant here because precisely the same four orbitals determine the diamagnetic global ring current in [MgP].[1] In the ipsocentric formulation,[7,8] the current induced in a molecule is ascribed wholly to perturbation of the wavefunction, with none of the complications generated by traditional formulations in terms of competing ground- and excited-state formal contributions. Current density, magnetic susceptibility and nuclear shieldings are then determined by the accessibility of excited electronic states of the system. In molecular orbital theory it is the allowed transitions between occupied and unoccupied orbitals that determine these properties, according to translation/rotation selection rules that determine the sense of the current.[8] Translational and electric dipole-moment selection rules are identical, whence the close correspondence between the electronic spectrum and the ring current of [MgP], where HOMO–LUMO transitions give essentially the whole of the diamagnetic global ring current.[1] Rotational and magnetic dipole-moment selection rules are identical, so that in $[MgP]^{2+}$ the $\Delta\lambda = 0$ HOMO–LUMO transition within the split $\lambda = 4$ pair ($3a_{2u}$ HOMO, $1a_{1u}$ LUMO) dominates the global paramagnetic ring current.

The orbital model gives a clear account of the sense of the ring currents in these systems. It can also explain the dependence of their spatial location on the charge of the central ion. Bifurcation of the global circulation across the pyrrole subunits is seen in the current density maps for porphin,[1] porphycene[2] and the expanded porphyrins sapphyrin and orangarin.[3] One intriguing observation from studies of this family of systems is that the *extent* of bifurcation of the global path depends not only on the structure of the macrocycle, but also on the charge at its centre.[4] Fig. 3 shows how the bifurcation changes when the central ion of [MgP] is replaced by a point charge $+Ze$ for (a) $Z = 0$, (b) $Z = 2$ and (c) $Z = 4$. The computed global current changes hardly at all when the central ion is replaced in the model system by charge $Z = 2$ {$j_{max} = 0.18$ a.u. for $Z = 2$ [Fig. 3(b)] *cf.* 0.17 a.u. with an explicit Mg^{2+} cation [Fig. 1(a)]}. Removal of this charge results in a substantial reduction in bifurcation in favour of the inner pathway [Fig. 3(a)], whilst replacement by charge $Z = 4$ again leads to reduction in bifurcation, but now in favour of the outer pathway [Fig. 3(c)]. A parallel pattern is observed for the paramagnetic ring currents of $[MgP]^{2+}$.

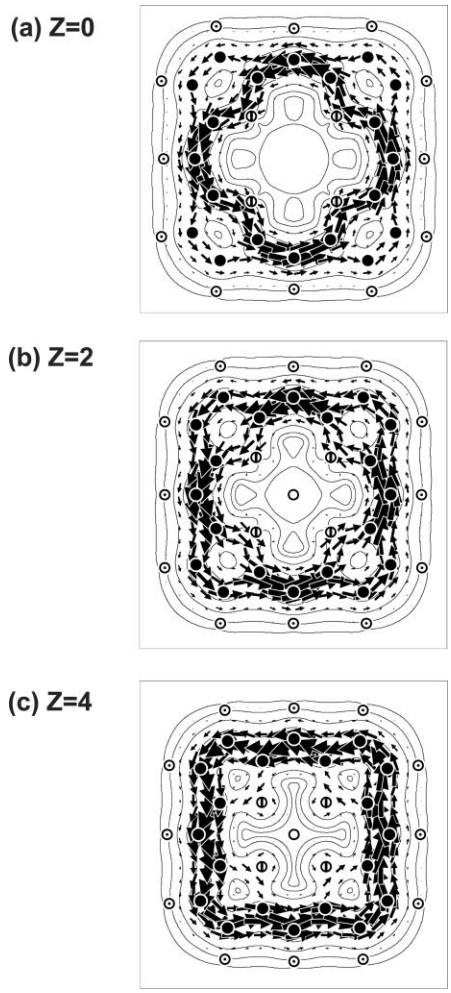

Fig. 3 Total π current density maps of model systems obtained from magnesium porphin by replacement of the central Mg^{2+} ion by charges Z_e for (a) $Z = 0$, (b) $Z = 2$, (c) $Z = 4$.

We show in the present paper how the orbital analysis of magnetic properties within the ipsocentric formulation of coupled Hartree–Fock theory[7,8] leads to a natural explanation of the changes in the global π ring currents arising from changes in the central charge. Results are presented for the model systems $[ZP^{2-}]$ and [ZP], in which P^{2-} is the (diatropic) porphin dianion and P is the (paratropic) neutral macrocycle, illustrating the influence of the central cation on the delocalisation pathway and ring current.

Unless there are specific orbital effects, an explanation of the behaviour of magnetically-induced currents in the presence of electric and magnetic fields can often be found, in the spirit of Larmor's interpretation of diamagnetism, in the principle that changes in current density follow changes in charge density.[15,16] In the ipsocentric approach, the current is governed by virtual transitions between occupied and unoccupied orbitals, and so strictly speaking it is the transition density rather than the density of the occupied orbital alone that should be considered.

In many cases, arguments based on charge and transition densities will lead to the same qualitative conclusion. In the present case, the non-uniform central field of the positive charge in the porphin ring gives rise to a two-way radial transfer of electronic charge within the π structure. Movement of the computed global π current, as Z increases from $Z = 0$, from an inner- to a bifurcated- to an outer-pathway can be interpreted in terms of a specific π shielding effect whereby electrons in high-lying π orbitals of each symmetry type are shielded from the centre by the electrons in the lower-lying orbitals of the same symmetry. The success of a simplified pseudo-π model in duplicating these effects shows that the changes in π structure are essentially independent of accompanying changes in the σ structure.

2. Computational details

The calculations of current density presented in this paper were performed with the 6-31G** Gaussian basis set by means of coupled Hartree–Fock theory within the ipsocentric (or CTOCD-DZ, continuous transformation of origin of current density-diamagnetic zero) formulation.[5–8] Geometries of all the systems were optimised with D_{4h} symmetry constraints at the RHF/6-31G** level. The π current density maps are plotted in a plane at $1a_0$ from that of the nuclei. Contours show the modulus of current density with values of 0.001×4^n a.u. (a.u. $= e\hbar/m_e a_0^4$), for $n = 0, 1, 2, \ldots$, and the arrows show the magnitude and direction of the projection of the current density vector in the plotting plane. Diatropic circulation is anticlockwise, paratropic clockwise, following the direction of circulation of the π electrons in a magnetic field at right angles to the molecular plane and pointing out of the map towards the viewer. Geometry optimisations were performed with CADPAC[17] and GAUSSIAN;[18] all other calculations with the SYSMO package.[19]

3. Orbital current density maps

The diatropic global ring current in the 'porphin dianion' series [ZP^{2-}] is dominated by contributions of the four electrons in the near-degenerate HOMO pair $1a_{1u}$ and $3a_{2u}$, and arises from virtual translational excitations to the $4e_g$ LUMO pair (Fig. 2). The orbital contributions, and their sum, are shown in Fig. 4 for $Z = 0$ (dianion), $Z = 2$ (modelling magnesium porphin), and $Z = 4$.

Comparison of the maps in the right-hand column of Fig. 4 with those in Fig. 3 confirms that the global π current is essentially the sum of the HOMO contributions. The orbital current densities show that the electrons in both orbitals contribute to the shift from inner to outer pathway, although not to the same extent. The effect is stronger in $3a_{2u}$, which has an almost exclusively inner pathway when $Z = 0$ and an outer pathway when $Z = 4$. For the $1a_{1u}$ orbital, there is some bifurcation even when $Z = 0$.

In the 'neutral porphin' series [ZP] the orbital $1a_{1u}$ is unoccupied and is the LUMO to its partner, the HOMO $3a_{2u}$. The

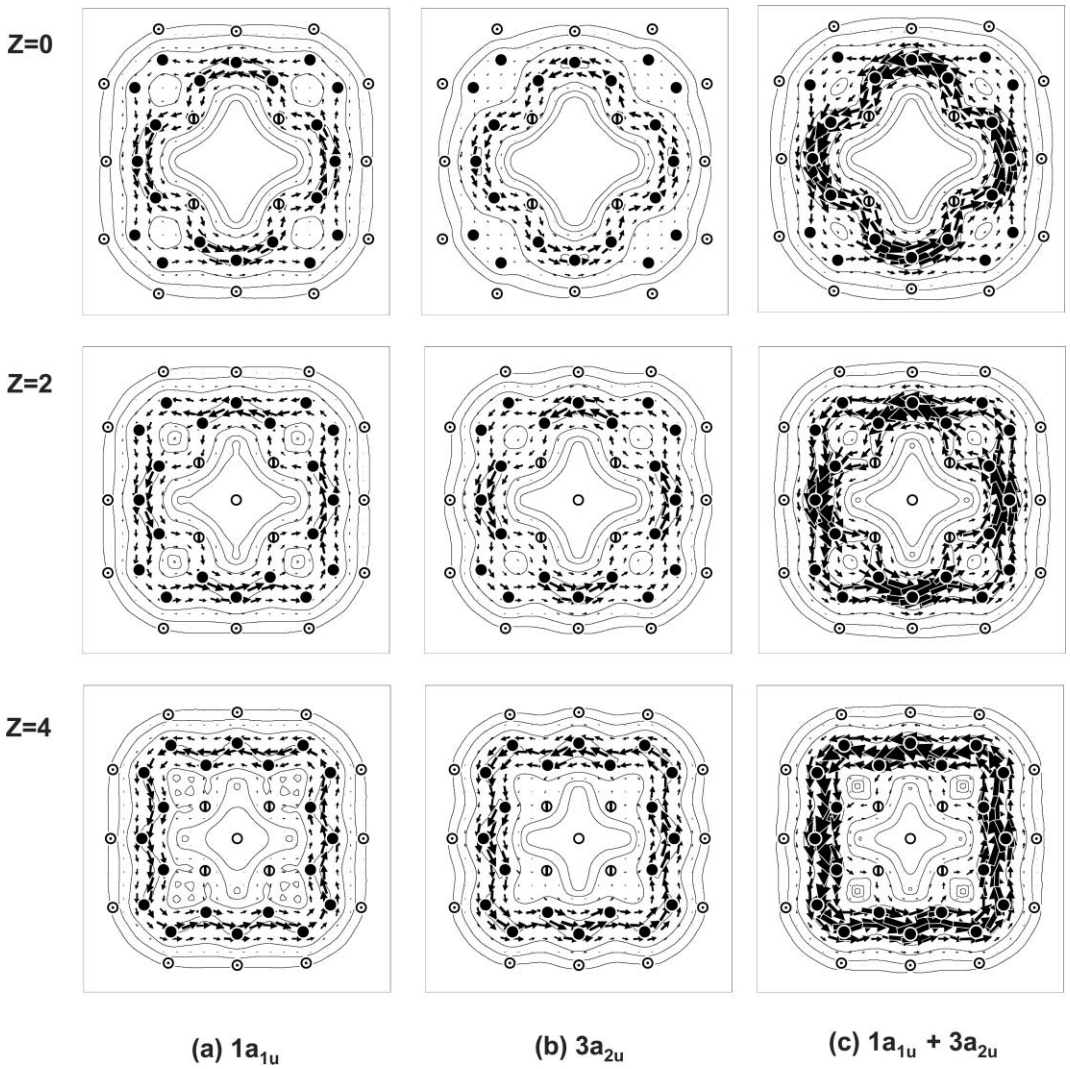

Fig. 4 Orbital π current density maps of the porphin dianion series [ZP^{2-}] for $Z = 0$, $Z = 2$ and $Z = 4$: (a) $1a_{1u}$, (b) $3a_{2u}$, and the sum of the orbital contributions (c) $1a_{1u} + 3a_{2u}$.

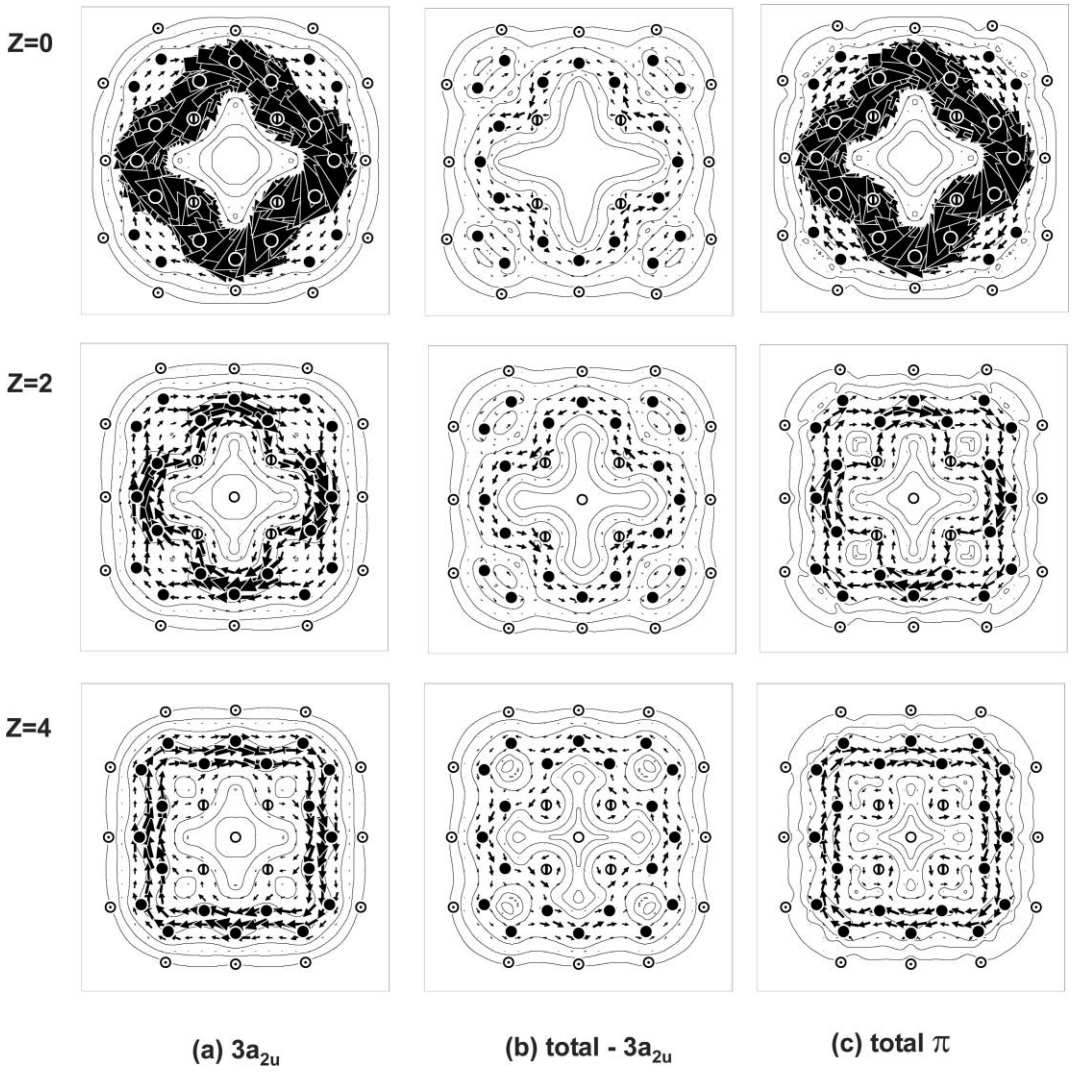

Fig. 5 Orbital π current density maps of the neutral porphin series [ZP] for $Z = 0$, $Z = 2$ and $Z = 4$: (a) $3a_{2u}$, (b) total π − $3a_{2u}$, and (c) total π.

[ZP] systems now display two-electron paramagnetism as a result of the rotationally-allowed transition $3a_{2u} \rightarrow 1a_{1u}$ between the partners. The electrons in the remaining orbitals form a closed-shell diatropic system, as shown in Figs. 5(b).

The most obvious feature of Fig. 5 is the large paratropic current for the $3a_{2u}$ orbital when $Z = 0$ (maximum current density $j_{max} = 0.37$ a.u., compared with 0.14 a.u. for $Z = 2$ and 0.12 a.u. for $Z = 4$). This enhanced value is partly due to a small HOMO–LUMO energy gap, but, as we will see, is mainly the result of particularly favourable rotational matching of the HOMO and LUMO orbitals in the region of the inner pathway.

More generally, the maps show an increase of current density in the outer pathway at the expense of the inner as the central charge increases. The central column of maps in Fig. 5 shows that a somewhat weaker *diatropic* contribution to the global ring current is also made by the electrons in the closed shell below the HOMO ($Z = 0$: $j_{max} = 0.06$ a.u., $Z = 2$: 0.07 a.u., $Z = 4$: 0.06 a.u.), with largest contribution coming from the four electrons in the $3e_g$ HOMO − 1 pair. A diatropic subsystem is a standard feature that accompanies the two-electron paratropicity associated with a split HOMO–LUMO pair.[8,20] In the present case, the diatropic subsystem has its origin in the translationally-allowed transitions to the vacated $1a_{1u}$, as well as with a lesser contribution from $2e_g$ and a paratropic contribution from $2a_{2u}$. These small contributions conspire to form weak localised circulations in the pyrrole units when $Z = 0$, which is absorbed in the global diatropic flow when $Z = 4$. Similar features have been observed in expanded porphyrins.[3]

As we have seen, the orbital model accounts for the overall features of the maps. An *explanation* of their charge dependence follows from inspection of changes in orbital densities, and a consideration of π shielding effects, as will be shown in the following section.

4. Orbital and density-difference maps

The HOMO π orbitals and an orbital of the LUMO pair in the porphin dianion series [ZP^{2-}] are shown in Fig. 6 for $Z = 0$, $Z = 2$ and $Z = 4$. It is clear that the two HOMO orbitals respond quite differently, and quite unexpectedly, to the central charge. Whilst orbital $1a_{1u}$ appears to remain almost unchanged as the charge increases from $Z = 0$, orbital $3a_{2u}$ shows a strong shift *away* from the increasing positive charge, from nitrogen onto peripheral CC bonds. The $4e_g$ LUMO also shows this outward shift, from nitrogen onto peripheral CC bonds.

The pattern of shifts is emphasised in Fig. 7 by the density-difference maps [$\psi^2(Z) - \psi^2(0)$], for $Z = 4$, for the HOMO orbitals and the LUMO pair. These difference maps have been obtained from computations at a common [MgP] geometry. The $1a_{1u}$ orbital shows the expected polarisation towards the central charge, but the shift is small and localised on carbons common to both inner and outer pathways. In contrast, the density-difference map for orbital $3a_{2u}$ shows marked polarisation away from the centre onto the periphery. The LUMO also moves towards the peripheral CC bonds at the expense of nitrogen.

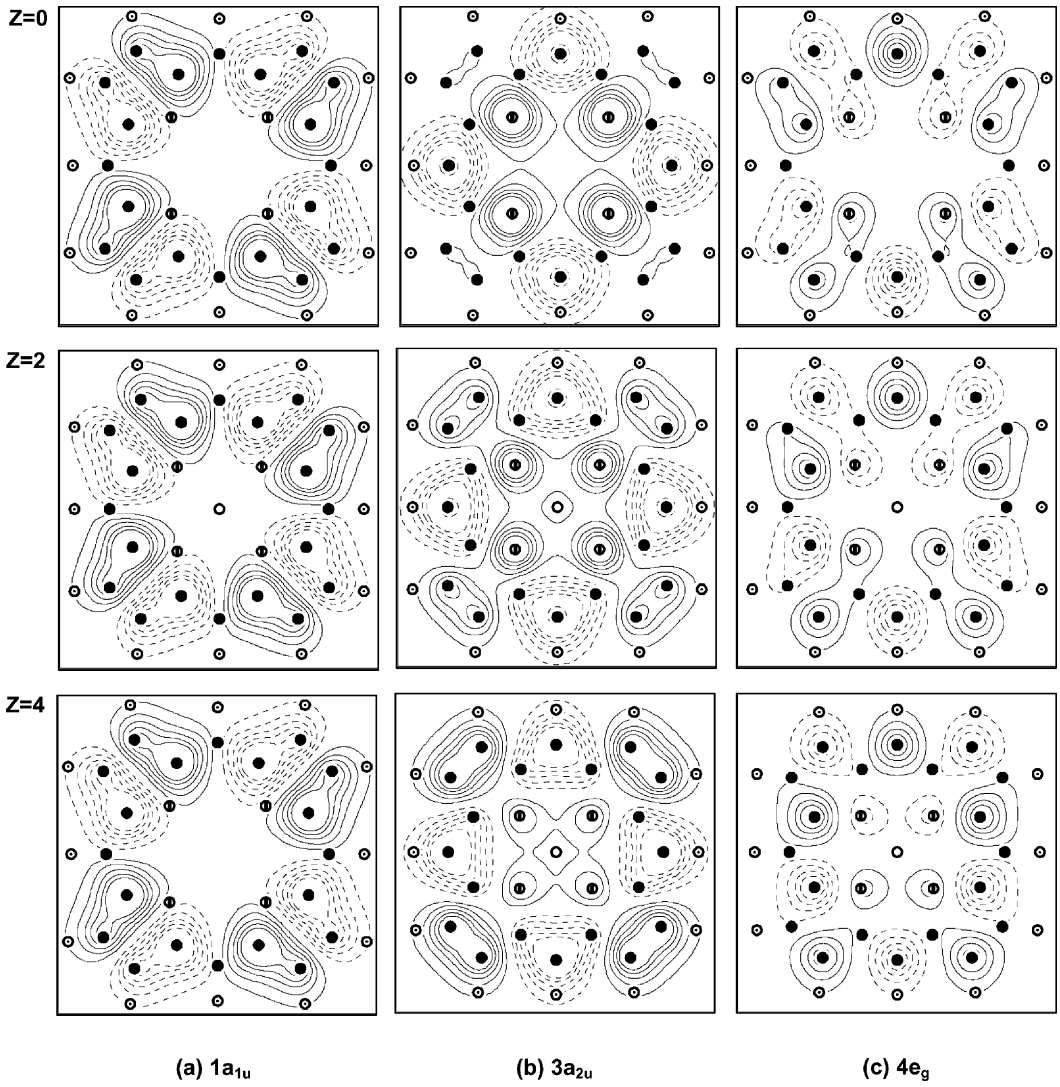

Fig. 6 HOMO and LUMO orbitals in the porphin dianion series [ZP^{2-}] for $Z = 0$, $Z = 2$ and $Z = 4$: (a) $1a_{1u}$, (b) $3a_{2u}$ and (c) one of the $4e_g$ pair. Contour values are $\pm 0.02 n a_0^{-3/2}$ for $n = 1, 2, 3, \ldots$ Solid and dashed lines denote positive and negative values, respectively.

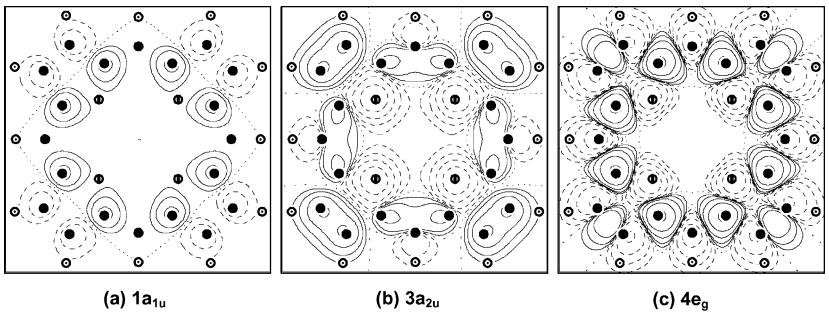

Fig. 7 Orbital density-difference maps $\psi^2(Z = 4) - \psi^2(Z = 0)$ of the porphin dianion series [ZP^{2-}]: for the HOMO (a) $1a_{1u}$ and (b) $3a_{2u}$ and the LUMO pair (c) $4e_g$. The contour values are $\pm 0.0001 \times 3^n a_0^{-3}$ for $n = 0, 1, 2, \ldots$ Solid lines show increase in charge density, dashed lines show decrease.

These observations on the orbitals and density differences are sufficient to explain the shift in orbital currents from inner to outer pathways in the series [ZP^{2-}] as the central charge Z is increased. In the case of $3a_{2u}$, the strong outward shift of the occupied orbital density from nitrogen onto the periphery, reinforced by that of the LUMO, results in a corresponding shift of current density onto the outer pathway. In the case of $1a_{1u}$, the occupied orbital spans both pathways with little change as Z increases, and it is the outward shift of the LUMO density that leads to the outward shift in current pathway.

In the series [ZP] orbital $3a_{2u}$ is the HOMO and its partner $1a_{1u}$ is the LUMO. These orbitals are similar to those shown in Fig. 6 for [ZP^{2-}], with orbital-density differences similar to those in Fig. 7. In this case, the LUMO is insensitive to changes of the central charge, and it is the outward shift of the $3a_{2u}$ HOMO that determines the pathway as Z increases. The magnitude of the paratropic current depends strongly on the rotational matching of HOMO and LUMO. Comparison of the two columns of Fig. 6, for $1a_{1u}$ and $3a_{2u}$, shows that a matching is obtained by rotation of either orbital through an angle $\pi/8$, appropriate

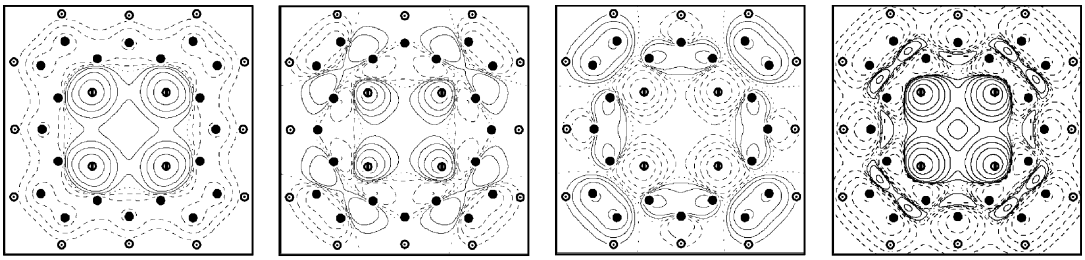

Fig. 8 Density-difference maps $\psi^2(Z=4) - \psi^2(Z=0)$ for the porphin dianion series $[ZP^{2-}]$, with $Z=4$, for orbitals (a) $1a_{2u}$, (b) $2a_{2u}$ and (c) $3a_{2u}$, and (d) for the total π charge density.

to a pair of orbitals with orbital angular momentum quantum number $\lambda = 4$. For $Z = 0$, this rotation gives strong overlap of the orbitals in regions along the inner pathway. As Z is increased, the overlap becomes progressively weaker as the $3a_{2u}$ density moves outward.

It remains to explain the computed shifts in the orbital densities themselves in the presence of the increasing central charge, and this is the point at which hypothesis (ii) of a π shielding or screening effect is invoked.

The hypothesis is that, whereas all the electrons are attracted to the central charge, there exists a specific π shielding effect whereby electrons in high-lying π orbitals of each symmetry type are shielded from the central charge by the electrons in the lower-lying orbitals of the same symmetry, resulting in a partial separation of charge within the π system. This arises in two ways: (a) electrostatic shielding, whereby an electron at a given radius is shielded from the centre by the electron density within that radius, and (b) radial orthogonality, whereby higher-lying orbitals are progressively excluded from the space occupied by lower-lying orbitals of the same symmetry, leading to a relative shift of orbital density away from the centre. The π shielding effect is closely analogous to the familiar nuclear shielding in atoms, with the screening constant increasing up the orbital ladder. Radial orthogonality, which applies to all orbitals, occupied and unoccupied, is already seen in the hydrogen atom, and for each symmetry results in an increasing number of radial nodes, as in the series 1s, 2s, 3s,..., with maximum orbital density at larger distances from the centre.

In the porphyrin macrocycle, the significant consequence of radial orthogonality is the shift of density from inner to outer pathway. This is demonstrated in Fig. 8 by density-difference maps $[\psi^2(Z) - \psi^2(0)]$ for the three occupied orbitals of symmetry a_{2u} in $[ZP^{2-}]$ with $Z = 4$. The lowest-lying orbital $1a_{2u}$ is polarised wholly towards the central charge, the second less so, and the third is polarised onto the perimeter. Fig. 8(d) also shows that the polarisation of the *total* π density is actually towards the central charge.

5. Pseudo-π calculations

The changes in the π structure arising from variation of the charge at the centre of the porphin macrocycle have been discussed without reference to the σ structure. That these changes are properties of the π structure alone, and occur independently of the σ structure, is confirmed by 'pseudo-π' model calculations. In the original pseudo-π method, a conjugated carbon framework is formally replaced by a set of hydrogen atoms bearing single 1s (STO-3G) orbitals.[21] Calculation within the ipsocentric formulation of the in-plane σ current density induced by a perpendicular magnetic field has been found to give a close numerical match to the out-of-plane π current density of the original carbon system at a height of $1a_0$, particularly when the original optimised geometry is used. For the present pseudo-π calculations of the porphyrin systems the difference between N and C has been ignored, a procedure that has a precedent in the 1950 Hückel calculations of Longuet-Higgins *et al*.[22] The total pseudo-π current density distributions computed in this way are shown in Fig. 9. The detailed agreement between the results of the pseudo-π and *ab initio* calculations of the π currents, shown in Fig. 3, suggests that the global behaviour of the ring current in the presence of a central charge does not depend in any essential way on possible changes in the σ structure. Studies of changes in the σ structure of the porphin macrocycle and of some simpler related systems in the presence of an electric field do suggest the presence of a corresponding σ shielding effect, but the analysis is complicated by the inherently localised nature of the σ structure.

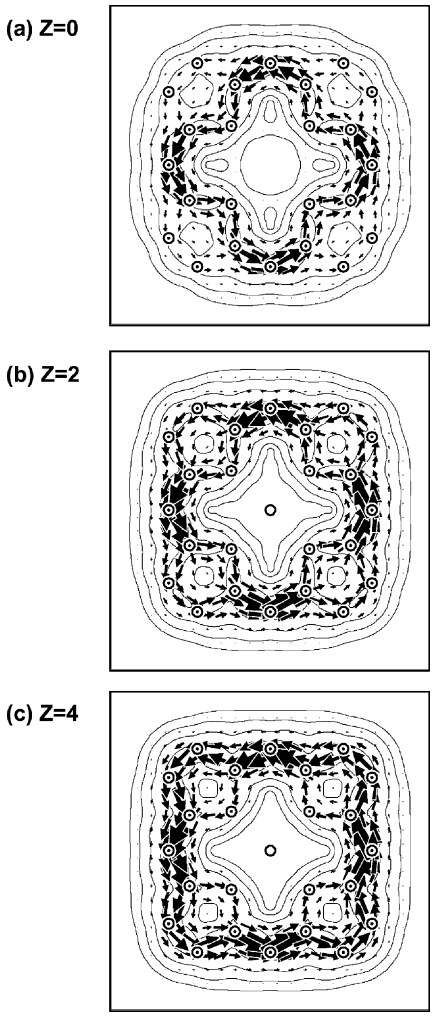

Fig. 9 Total pseudo-π current density maps of $[ZP^{2-}]$ for (a) $Z = 0$, (b) $Z = 2$, (c) $Z = 4$.

6. Conclusion

The ipsocentric method and its associated orbital model can explain the sense of the global ring current circulation in porphin macrocycles and also the way in which the current pathway varies with the change of the central cation. Although perhaps apparently counterintuitive, the movement of current arising from an increasing central charge is predicted by a two-dimensional shielding model. For molecular design purposes, it may be noted that variation of the central cation/charge could therefore be used to tune the pathway of the ring current and π delocalisation in porphyrins, and hence adjust the local magnetic fields, chemical shifts and magnetic susceptibility anisotropy.

References

1 E. Steiner and P. W. Fowler, *Chem. Phys. Chem.*, 2002, **3**, 114–116.
2 E. Steiner and P. W. Fowler, *Org. Biomol. Chem.*, 2003, **1**, 1785–1789.
3 E. Steiner and P. W. Fowler, *Org. Biomol. Chem.*, 2004, **2**, 34–37.
4 E. Steiner and P. W. Fowler, 'Mapping the Global Ring Currents in Porphyrins and Chlorins', in *Chlorophylls and Bacteriochlorophylls: Biochemistry Biophysics and Biological Function*, B. Grimm, R. Porra, W. Rüdiger and H. Scheer, eds., Advances in Photosynthesis, Springer, 2005, in press.
5 T. Keith and R. F. W. Bader, *Chem. Phys. Lett.*, 1993, **210**, 223–231.
6 P. Lazzeretti, M. Malagoli and R. Zanasi, *Chem. Phys. Lett.*, 1994, **220**, 299–304.
7 E. Steiner and P. W. Fowler, *, J. Phys. Chem. A*, 2001, **105**, 9553–9562.
8 E. Steiner and P. W. Fowler, *Chem. Commun.*, 2001, 2220–2221.
9 J. W. Buchler, in *Porphyrins and Metalloporphyrins*, K. E. Smith, ed., Elsevier, Amsterdam & New York, 1975, pp. 399–514.
10 N. B. McKeown, *Phthalocyanine Materials*, (Chemistry of Solid State Materials 6), Cambridge University Press, Cambridge, 1998.
11 J. L. Sessler and S. J. Weghorn, *Expanded, Contracted and Isomeric Porphyrins*, (Pergamon Tetrahedron Organic Chemistry Series 15), Elsevier, Amsterdam, 1997.
12 J. Dalton, *notebook*, 3 Sep. 1803, *A new system of chemical philosophy*, Manchester, 1808.
13 E. Rabinowitch, *Rev. Mod. Phys.*, 1944, **16**, 226–235.
14 M. Gouterman, *J. Chem. Phys.*, 1959, **30**, 1139–1161.
15 A. Soncini and P. W. Fowler, *Chem. Phys. Lett.*, 2004, **400**, 213–220.
16 A. Soncini, P. W. Fowler and F. Zerbetto, *Chem. Phys. Lett.*, 2005, **405**, 136–141.
17 R. D. Amos and J. E. Rice, *The Cambridge Analytical Derivatives Package, issue 4.0*, 1987.
18 *Gaussian 98, Revision A.6*, M. J. Frisch, G. W. Trucks, H. B. Schlegel, G. E. Scuseria, M. A. Robb, J. R. Cheeseman, V. G. Zakrzewski, J. A. Montgomery, Jr., R. E. Stratmann, J. C. Burant, S. Dapprich, J. M. Millam, A. D. Daniels, K. N. Kudin, M. C. Strain, O. Farkas, J. Tomasi, V. Barone, M. Cossi, R. Cammi, B. Mennucci, C. Pomelli, C. Adamo, S. Clifford, J. Ochterski, G. A. Petersson, P. Y. Ayala, Q. Cui, K. Morokuma, K. Malick, A. D. Rabuck, K. Raghavachari, J. B. Foresman, J. Cioslowski, J. V. Ortiz, B. B. Stefanov, G. Liu, A. Liashenko, P. Piskorz, I. Komaromi, R. Gomperts, R. L. Martin, D. J. Fox, T. Keith, M. A. Al-Laham, C. Y. Peng, A. Nanayakkara, C. Gonzalez, M. Challacombe, P. M. W. Gill, B. Johnson, W. Chen, M. W. Wong, J. L. Andres, C. Gonzalez, M. Head-Gordon, E. S. Replogle and J. A. Pople, Gaussian, Inc., Pittsburgh, PA, 1998.
19 P. Lazzeretti and R. Zanasi, *SYSMO Package*, University of Modena, Italy, 1980; E. Steiner, P. W. Fowler, R. W. A. Havenith and A. Soncini, *Additional routines for evaluation and plotting of current density*, University of Exeter, YEAR?.
20 P. W. Fowler, R. W. A. Havenith, L. W. Jenneskens, A. Soncini and E. Steiner, *Angew. Chem., Int. Ed.*, 2002, **41**, 1558–1560.
21 P. W. Fowler and E. Steiner, *Chem. Phys. Lett.*, 2002, **364**, 259–266.
22 H. C. Longuet-Higgins, C. W. Rector and J. R. Platt, *J. Chem. Phys.*, 1950, **18**, 1174–1181.